

## Study of 2-thiocytosine/ surfactant adsorption at the R-AgLAFe/chlorate(VII) interface – impact of surfactant ionic character

Marlena Martyna <sup>1</sup>, Mariusz Grochowski <sup>1</sup>, Teresa Urban <sup>2</sup>, Agnieszka Nosal-Wiercińska <sup>1</sup>

<sup>1</sup> Department of Analytical Chemistry, Institute of Chemical Sciences, Faculty of Chemistry, Maria Curie-Skłodowska University, Maria Curie-Skłodowska Sq. 3, 20-031 Lublin, Poland

<sup>2</sup> Department of Radiochemistry and Environmental Chemistry, Institute of Chemical Sciences, Faculty of Chemistry, Maria Curie-Skłodowska University in Lublin, M. Curie-Skłodowska Sq. 3, 20-031 Lublin, Poland

Corresponding author: [agnieszka.nosal-wiercinska@mail.umcs.pl](mailto:agnieszka.nosal-wiercinska@mail.umcs.pl) (Agnieszka Nosal-Wiercińska)

**Abstract:** Effect of 2 - thiocytosine on the parameters of double R-AgLAFe/ chlorate(VII) interface layer in the presence of different surfactants has been studied. There were determined the adsorption parameters such as: differential capacity of the double layer ( $C_d$ ) at the R-AgLAFe/ basic electrolyte interface; potential of zero charge ( $E_z$ ) and surface tension at the potential of zero charge ( $\gamma_z$ ). The predominance of 2-thiocytosine in formation of adsorption equilibria of 2-thiocytosine-SDS and 2-thiocytosine-CTAB mixtures as well as the competitive adsorption between molecules 2-thiocytosine-surfactant or mixed micelles was proved. The changes pointing out to different arrangement of SDS or CTAB molecules on the electrode surface also in the presence of 2-thiocytosine were observed.

**Keywords:** mixed adsorption layers, 2 - thiocytosine, SDS, CTAB, adsorption parameters, R-AgLAFe electrode

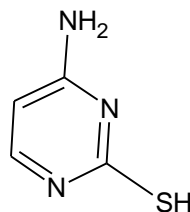
### 1. Introduction

Adsorption processes play an important role in the phenomena occurring at the phase interfaces. This could be used to develop an effective layer for prevention from corrosion effects. Continuous renewal of barrier layers is costly, time-consuming, and frequently contributes to pollution of the environment. For that reason, this is a global problem which requires quick solution. Adsorbed species at the metal/solution interface can change the rate of corrosion.

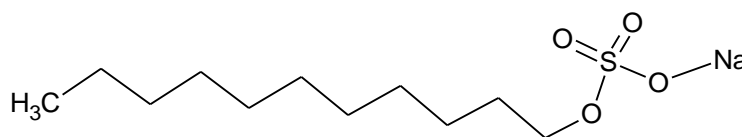
Adsorption of sulphur-containing molecules from the solutions on metals forming closely packed and oriented monolayers provide a convenient method for assigning desired chemical or physical properties of the surface (Dubois et al., 1992; Ulman, 1996). Using a mixture of adsorbates, it is possible to introduce various chemical functional properties on the surface (Bertilsson et al., 1993; J. P. Folkers et al., 1994; Gugęła-Fekner et al., 2015; Szymczyk et al., 2015). The most intensive and extensive investigations were carried on the mercury electrode. Electrode surface properties are substantially modified by the adsorbed molecules which affect the electrode reactions significantly. This is of significant importance and application in the processes of metals electrodeposition, molecular and biomolecular electronics as well as in the studies on biological membranes or inspection and optimization of the conditions e.g. in the drugs release mechanisms.

Surfactants undergo physical adsorption and achieving the critical micellization concentrations they form multidimensional micelles leading to the multilayer adsorption. The adsorption equilibria, which are formed with the predominance of the organic substance, and the competitive adsorption in the mixed adsorption layers were proved (Chen et al., 2017; Diehl et al., 1996; Gugęła-Fekner et al., 2015; Avranas et al., 2000; Nosal – Wiercińska et al., 2018).

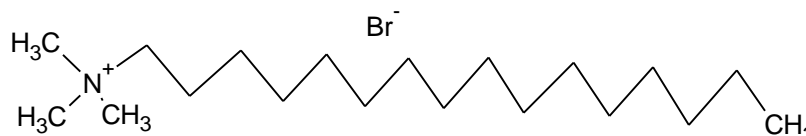
The results presented in this paper concern the study of the mixed adsorption layers of 2-thiocytosine–sodium 1-decanesulfonate and 2-thiocytosine–hexadecyltrimethylammonium bromide (Scheme 1 – 3).



Scheme 1. 2-thiocytosine



Scheme 2. Sodium 1-decanesulfonate (SDS)



Scheme 3. Hexadecyltrimethylammonium bromide(CTAB)

The novel cyclically renewable liquid silver amalgam film electrode (R-AgLAFe) (Nosal-Wiercińska et al., 2021) applied in the studies enabled as accurate determination of adsorption parameters (differential capacity  $C_d$  of the double layer) as the mercury electrode. The issue of environmental protection associated with the reduction of toxic mercury indispensable for formation of silver amalgam film as well as the generated waste is of significant importance (Nosal-Wiercińska et al., 2021).

## 2. Materials and methods

The surfactant and 2-thiocytosine solutions were prepared from Fluka reagents directly before the measurements. The concentration of sodium 1-decanesulfonate was in the range from  $1 \cdot 10^{-5}$  to  $9 \cdot 10^{-5}$  mol·dm<sup>-3</sup> whereas that of hexadecyltrimethylammonium bromide was ranged from  $1.5 \cdot 10^{-6}$  to  $1.5 \cdot 10^{-5}$  mol·dm<sup>-3</sup>. The concentration of the 2-thiocytosine was chosen to be  $1 \cdot 10^{-3}$  mol·dm<sup>-3</sup>. The supporting electrolyte was  $0.5 \text{ mol} \cdot \text{dm}^{-3} \text{ NaClO}_4 + 0.5 \text{ mol} \cdot \text{dm}^{-3} \text{ HClO}_4$  due to the weak complex-forming properties of ClO<sub>4</sub><sup>-</sup> ions and the fact of their weak adsorption on the mercury surface.

The solutions were deaerated using nitrogen, which was passed over the solution during the measurements.

The impedance measurements were performed using an AUTOLAB electrochemical analyzer controlled by the GPES software (Version 4.9) (Eco Chemie, Utrecht Netherlands). The cell stand included a three-electrode system with a cyclically renewable liquid silver amalgam film electrode (R-AgLAFe) refreshed before each measurement with a surface area of 17.25 mm<sup>2</sup> used as a working electrode; a silver/silver chloride electrode (Ag/AgCl, 3 MKCl) as a reference electrode; and a Pt wire as a counter electrode. The silver base for the amalgam film electrode was prepared from the 0.5 mm diameter polycrystalline silver wire of 99.999% purity (Alfa Aesar, A. Johnson Matthey Company, Germany).

Viscosity measurements were performed using the rotational CVO 50 rheometer with the “double gap” measuring system (Bohlin Instruments).

The critical micelle concentration (CMC) was determined by the viscosity method. The measurements were made in  $1 \text{ mol dm}^{-3}$  chlorate(VII)–SDS,  $1 \text{ mol dm}^{-3}$  chlorate(VII)–CTAB systems and in the

presence of 2-thiocytosine. In the range of studied concentrations CMC was determined from the dependence of viscosity of the solutions on their concentrations. At the concentration corresponding to CMC a rapid change of system viscosity was observed (Nosal-Wiercińska et al., 2018).

The differential capacity of the double layer,  $C_{dl}$ , at the R-AgLAFe/supporting electrolyte interface was determined for the whole polarisation range, the capacity dispersion was tested at different frequencies between 200 and 1000 Hz. As a result of the differential capacitance extrapolation to zero frequency, the differential capacity curves corresponding to the adsorption equilibrium were obtained.

This procedure assumes that the impedance of the double layer is equivalent to a series of capacity-resistance combinations and the rate of adsorption is diffusion – controlled (Nosal-Wiercińska, 2010).

The potential of zero charge  $E_z$  was determined using a streaming electrode (Nosal-Wiercińska, 2010) with the accuracy of  $\pm 0.1$  mV. The surface tension at the potential of zero charge  $\gamma_z$  was measured using the method of the highest pressure inside the mercury drop presented by Schiffrin (Nosal-Wiercińska, 2010).

The surface tension values were determined with an accuracy of  $\pm 0.2$  mN·m<sup>-1</sup>.

### 3. Results and discussion

#### 3.1. Differential capacity curves

The previous studies proved the adsorption of 2-thiocytosine on the cyclically renewable liquid silver amalgam film electrode (R-AgLAFe) (Josypc̣uk et al., 2013; Nosal – Wiercińska et al., 2021). As for the adsorption of 2-thiocytosine, it was related to the adsorption form RS-Hg, which was created due to mercury electrooxidation (Josypc̣uket al., 2013). The range of potentials between the adsorption and desorption peaks made an area of labile adsorption of RS-Hg on the amalgam electrode (Nosal – Wiercińska et al., 2021).

Figs. 1 and 2 show the capacitance curves in 1 mol·dm<sup>-3</sup> chlorates(VII) in the presence of anionic detergent sodium 1-decanesulfonate (Fig. 1) and cationic detergent hexadecyltrimethylammonium bromide (Fig. 2). In the region of the “hump” potentials, appearing in 1 mol·dm chlorate(VII) without the studied substances ( $\approx -0.3$  –  $-0.8$  V), after the addition of SDS to the solution, the height of the “hump” decreases (Fig. 1). A reverse dependence was observed in the presence of the basic electrolyte CTAB (Fig. 2). Such different arrangement of capacity curves may result from the differences in the interactions, mainly electrostatic ones, of adsorbed detergent molecules (which possess different charges) (Pagac et al., 1998; Klin et al., 2011).

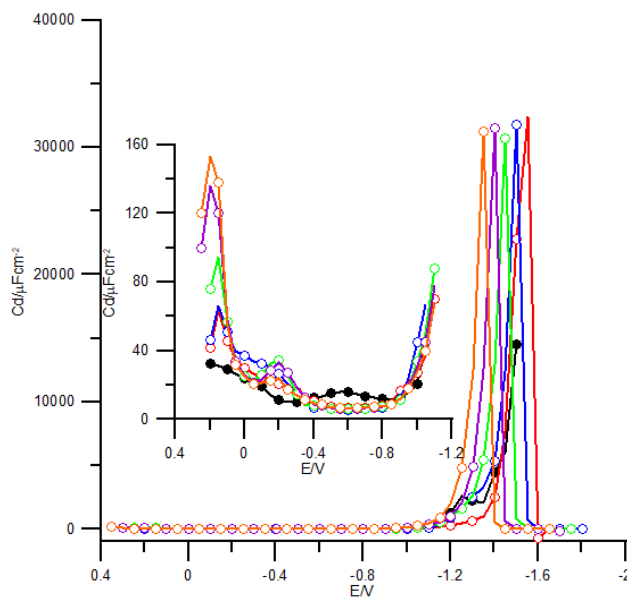


Fig. 1. Differential capacity – potential curves of the double layer interface R-AgLAFe / 1 mol·dm<sup>-3</sup> chlorate(VII) with various concentrations of SDS: (●) 0, (○)  $1.5 \cdot 10^{-5}$ , (○)  $3 \cdot 10^{-5}$ , (○)  $5 \cdot 10^{-5}$ , (○)  $7.5 \cdot 10^{-5}$ , (○)  $9 \cdot 10^{-5}$  (in mol·dm<sup>-3</sup>)

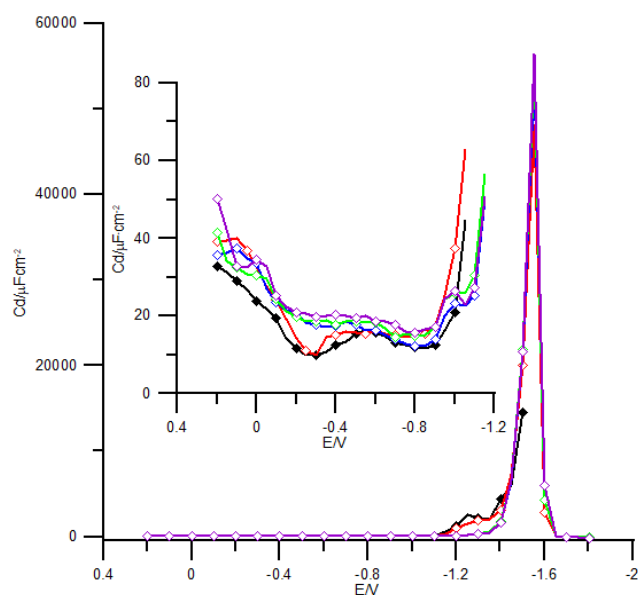


Fig. 2. Differential capacity - potential curves of the double layer interface R-AgLAFe / 1 mol·dm<sup>-3</sup> chlorate(VII) with various concentrations of CTAB: (♦) 0, (◇) 1.5·10<sup>-6</sup>, (◊) 3·10<sup>-5</sup>, (◊) 6·10<sup>-5</sup>, (◇) 1.5·10<sup>-5</sup> (in mol·dm<sup>-3</sup>)

In the region of higher potentials ( $\approx 0.2$  V) the adsorption peaks occur in the presence of SDS (Fig. 1) with the increasing surfactant concentration in the solution. At definitely negative potentials (about  $-1.5$  V) the reappear desorption peaks which do not change their height with the increasing surfactant concentrations in the basic electrolyte solution. However, they change their position shifting towards the less negative potentials (for the concentration  $9 \cdot 10^{-5}$  mol·dm<sup>-3</sup> SDS the desorption peak appears at about  $-1.3$  V).

In the region of higher potentials ( $\approx 0.1$  V) only a small outline of the adsorption peaks is observed in the presence of CTAB (Fig. 2) but in the area of the most negative potentials about  $-1.5$  V the desorption peak appears. This is very sharp peak increase with the increasing concentration of adsorbate in the basic solution electrolyte.

Considering such different depiction of the capacitance curves obtained for the tested surfactants and based on the literature data, it can be concluded that at the molecular level the surfactants molecules have titled orientation with most of their hydrophobic segment in contact with the mercury surface and their hydrophilic segment facing the aqueous solution (Avranas et al., 2000).

It should be mentioned that in the range of studied concentrations for the cationic detergent, the critical micelle concentration CMC was not observed. However, in the case of the anionic surfactant its value is  $3 \cdot 10^{-5}$  mol·dm<sup>-3</sup> SDS. The electrode potential change is followed by reorganization of the adsorption layers SDS within two surface structures, namely the two-layer and three-layer micelles (Sotiropoulos et al., 1993; Kumar et al., 2019).

Fig. 3 presents the differential capacity curves obtained experimentally in 1 mol dm<sup>-3</sup> chlorate(VII) in the presence of  $1 \cdot 10^{-3}$  mol·dm<sup>-3</sup> 2-thiocytosine and with the addition of chosen SDS concentration. The addition of the surfactant to the basic electrolyte solution containing 2-thiocytosine does not change the picture of capacity curves (Nosal - Wiercińska et al., 2021). It should be noticed that the increase in the SDS concentration in the basic electrolyte results in the evident decrease of adsorption and desorption peaks. Addition of SDS influences the change of the desorption peak potential shifting it towards less negative values. This can be associated with the effect of the anionic SDS molecule in formation of adsorption equilibria. However, the interactions of 2-thiocytosine molecules and the surfactant resulting in formation of a more or less compact structure of mixed adsorption layer can not be excluded (Gugała-Fekner et al., 2015; Nosal - Wiercińska et al., 2018; Klin et al., 2011). Moreover, in the presence of CTAB in the basic electrolyte solution containing  $1 \cdot 10^{-3}$  mol·dm<sup>-3</sup> of 2-thiocytosine there are observed some changes in the area of adsorption peak which evidently increases with the increasing concentration of CTAB (Fig. 4). As CTAB is a cationic molecule, one can expect its different arrangement on the electrode surface. Definitely one can observe the change of structure and properties

of the adsorption layer at the R-AgLAFe/aqueous chlorate(VII) solution in the presence of 2-thiocytosine and CTAB solution which results in the mixed adsorption layer formation (Gugała-Fekner et al., 2015; Nosal – Wiercińska et al., 2018; Klin et al., 2011). The analysis of Figs. 3 and 4 shows a distinct predomination of 2-thiocytosine in the adsorption equilibria formation (Nosal – Wiercińska et al., 2018).

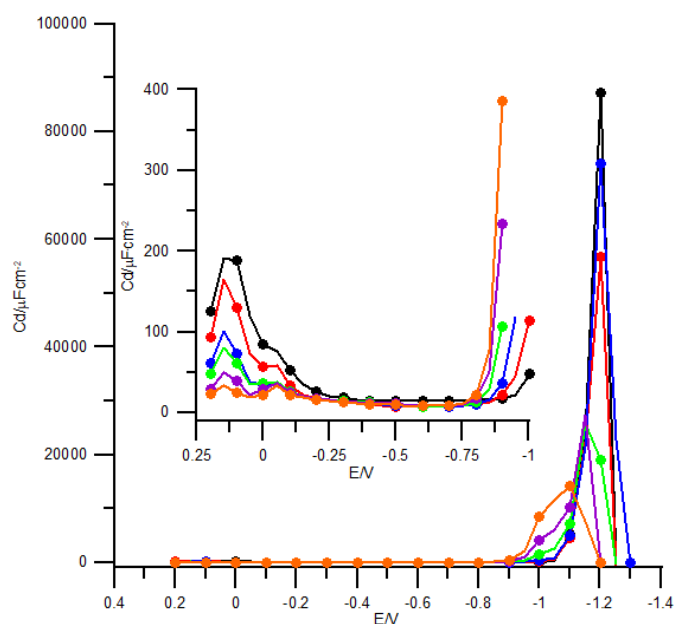


Fig. 3. Differential capacity - potential curves of the double layer interface R-AgLAFe / 1 mol·dm<sup>-3</sup> chlorate(VII) with 1·10<sup>-3</sup> mol·dm<sup>-3</sup> 2-thiocytosine and with various concentrations of SDS: (●) 0, (●) 1.5·10<sup>-5</sup>, (●) 3·10<sup>-5</sup>, (●) 5·10<sup>-5</sup>, (●) 7.5·10<sup>-5</sup>, (●) 9·10<sup>-5</sup> (in mol·dm<sup>-3</sup>)

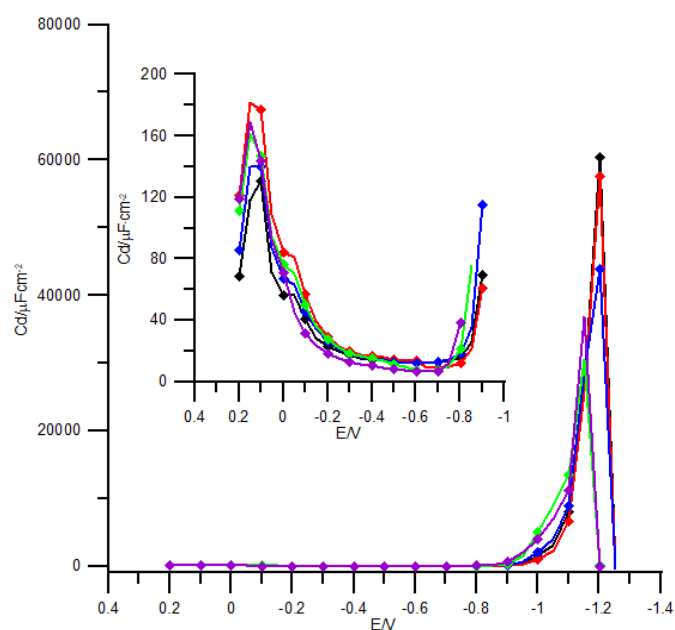


Fig. 4. Differential capacity - potential curves of the double layer interface R-AgLAFe / 1 mol·dm<sup>-3</sup> chlorate(VII) with 1·10<sup>-3</sup> mol·dm<sup>-3</sup> 2-thiocytosine and with various concentrations of CTAB: (◆) 0, (◆) 1.5·10<sup>-6</sup>, (◆) 3·10<sup>-5</sup>, (◆) 6·10<sup>-5</sup>, (◆) 1.5·10<sup>-5</sup> (in mol·dm<sup>-3</sup>).

### 3.2. Potentials of zero charge and the surface tension

Tables 1-5 present the values of the potentials of zero charge  $E_z$  and the values of the surface tension  $\gamma_z$  at the zero charge potential for the studied systems.

As follows from Table 1 the addition and increase of 2-thiocytosine concentration in the 1 mol · dm<sup>-3</sup> chlorates(VII) solution causes shift of  $E_z$  towards more positive potentials.

The dependences are linear which points out to the specific adsorption of 2-thiocytosine on mercury (Avranas et al., 2000; Sotiropoulos et al., 1993; Kumar et al., 2019). Due to similar properties of mercury and amalgam electrodes (Baš et al., 2010) as well as analogous mechanisms of action on them (Brycht et al., 2014), one can refer to it as the specific adsorption of TC also as regards the R-AgLAFe electrode. The presence of surfactants in the 1 mol · dm chlorates(VII) solution also affects the changes in the  $E_z$  values (Tables 2 and 3).

The addition of SDS results in the shift of  $E_z$  towards the positive potentials. However, it should be noted that for the concentration of CMC  $3 \cdot 10^{-5}$  mol · dm<sup>-3</sup> these changes are severe and may indicate the aggregation phenomena at the Hg-aqueous electrolyte solution interphase in the presence of surfactant (Pagac et al., 1998). However, in the case of CTAB there are observed evidently reverse dependences and the addition of surfaktant shifts  $E_z$  towards the positive potentials but successive increase of concentrations causes a shift of the zero charge potential value towards the negative potentials which indicates the adsorption of CTAB oriented with the negative end towards the mercury surface (Brycht et al., 2014).

Table 1. The potential of zero - charge  $E_z$  vs. Ag/AgCl electrode and surface tension  $\gamma_z$  for  $E_z$  of 1 mol · dm<sup>-3</sup> chlorates(VII) solutions + different 2-thiocytosine systems

$10^4 c_{2\text{-thiocytosine}} / \text{mol} \cdot \text{dm}^{-3}$	$- E_z / \text{V}$	$\gamma_z / \text{m N m}^{-1}$
0.00	0.480	477.5
1.00	0.465	477.0
5.00	0.457	476.0
10.0	0.445	475.0
50.0	0.439	473.0
100.0	0.435	472.0

Table 2. The potential of zero - charge  $E_z$  vs. Ag/AgCl electrode and surface tension  $\gamma_z$  for  $E_z$  of 1 mol · dm<sup>-3</sup> chlorates(VII) solutions + different SDS surfactant concentration systems; (CMC underlined)

$10^5 c_{\text{SDS}} / \text{mol} \cdot \text{dm}^{-3}$	$- E_z / \text{V}$	$\gamma_z / \text{m N m}^{-1}$
0.0	0.480	477.5
0.6	0.476	514.6
1.5	0.475	512.6
<u>3.0</u>	<u>0.435</u>	<u>511.5</u>
5.0	0.427	511.0
7.5	0.420	510.5
9.0	0.415	508.5

Table 3. The potential of zero - charge  $E_z$  vs. Ag/AgCl electrode and surface tension  $\gamma_z$  for  $E_z$  of 1 mol · dm<sup>-3</sup> chlorates(VII) solutions + different CTAB surfactant concentration systems

$10^5 c_{\text{CTAB}} / \text{mol} \cdot \text{dm}^{-3}$	$- E_z / \text{V}$	$\gamma_z / \text{m N m}^{-1}$
0.00	0.480	477.5
0.075	0.446	516.6
0.15	0.449	515.1
0.30	0.459	514.6
0.60	0.466	513.6
1.50	0.469	513.6
3.00	0.475	512.6

Table 4. The potential of zero - charge  $E_z$  vs. Ag/AgCl electrode and surface tension  $\gamma_z$  for  $E_z$  of 1 mol·dm<sup>-3</sup> chlorates(VII) solutions + 1·10<sup>-3</sup> mol·dm<sup>-3</sup> 2-thiocytosine + different SDS surfactant concentration systems; (CMC underlined)

$10^5 c_{\text{SDS}} / \text{mol} \cdot \text{dm}^{-3}$	$- E_z / \text{V}$	$\gamma_z / \text{m N m}^{-1}$
0.0	0.435	472.0
0.6	0.466	503.5
1.5	0.465	504.5
3.0	0.462	501.5
<u>5.0</u>	<u>0.401</u>	<u>500.5</u>
7.5	0.352	499.5
9.0	0.335	497.5

Table 5. The potential of zero - charge  $E_z$  vs. Ag/AgCl electrode and surface tension  $\gamma_z$  for  $E_z$  of 1 mol·dm<sup>-3</sup> chlorates(VII) solutions + 1·10<sup>-3</sup> mol·dm<sup>-3</sup> 2-thiocytosine + different CTAB surfactant concentration systems

$10^5 c_{\text{CTAB}} / \text{mol} \cdot \text{dm}^{-3}$	$- E_z / \text{V}$	$\gamma_z / \text{m N m}^{-1}$
0.00	0.435	472.0
0.075	0.457	504.5
0.15	0.466	503.5
0.30	0.468	502.5
0.60	0.470	501.5
1.50	0.475	500.5
3.00	0.479	499.5

For the mixed adsorption layers 2-thiocytosine-SDS is observed the shift of the values  $E_z$  towards more positive z potentials. However, for the concentration  $5 \cdot 10^{-5}$  mol·dm<sup>-3</sup>(CMC), the shifts are evidently larger which can be explained by competitive adsorption or coadsorption of 2-thiocytosine-SDS or mixed micelles (Gugała-Fekner et al., 2015; Nosal-Wiercińska et al., 2018). For the mixed adsorption layers 2-thiocytosine-CTAB the values  $E_z$  shift towards more negative potentials. Thus, the addition of the cationic surfactant to the basic electrolyte solution containing 2-thiocytosine does not cause reorganization in the CTAB arrangement on the mercury surface.

The values of surface tension  $\gamma_z$  at the zerocharge potential (Tables 1 - 5) decrease for all studied systems as proved by the adsorption phenomenon (Nosal-Wiercińska et al., 2018; Nosal-Wiercińska, 2010).

#### 4. Conclusions

The adsorption studies indicate a change in the structure and properties of the adsorption layer at the R-Ag/LAFe/aqueous chlorate(VII) solution interface in the presence of the mixtures of 2-thiocytosine and SDS as well as 2-thiocytosine and CTAB which results in the formation of the mixed adsorption layer.

The predominance of 2-thiocytosine in formation of adsorption equilibria of 2-thiocytosine-SDS and 2-thiocytosine-CTAB mixtures as well as the competitive adsorption between the 2-thiocytosine - surfactant molecules or mixed micelles were proved. The ClO<sub>4</sub><sup>-</sup> ions should not be neglected in these interactions. Due to the fact that SDS and CTAB are different molecules considering their charge (SDS is anionic but CTAB is cationic), there were observed some changes indicating different arrangement of these molecules on the electrode surface also in the presence of 2-thiocytosine.

#### References

- AVRANAS, A., PAPADOPOULOS, N., PAPOUTSI, D., SOTIROPOULOS, S., 2000. Adsorption of the neutral macromonomeric surfactant Tween - 80 at the mercury/electrolyte solution interface as a function of electrode potential and time, *Langmuir*, 16, 6043-6053.

- BAŚ, B., BAŚ, S., 2010. *Rapidly renewable silver amalgam annular band electrode for voltammetry and polarography*, *Electrochem. Commun.*, 12, 816-819.
- BERTILSSON, L., LIEDBERG, B., 1993. *Infrared study of thiol monolayer assemblies on gold: preparation, characterization, and functionalization of mixed monolayers*. *Langmuir*, 9, 141-149.
- BRYCHT, M., SKRZYPEK, S., NOSAL-WIERCIŃSKA, A., SMARZEWSKA, S., GUZIEJEWSKI, D., CIESIELSKI, W., BURNAT, B., LENIART, A., 2014. *The new application of renewable silver amalgam film electrode for the electrochemical reduction of nitrile, cyazofamid, and its voltammetric determination in the real samples and in a commercial formulation*. *Electrochim. Acta*, 134, 302-308.
- CHEN, X., MCCRUM, I. T., SCHWARZ, K. A., JANIK, M. J., KOPER, M. T., 2017. *Co-adsorption of cations as the cause of the apparent pH dependence of hydrogen adsorption on a stepped platinum single-crystal electrode*. *Angew. Chem. Int. Ed.*, 56, 15025-15029.
- DIEHL, R. D., MCGRATH, R., 1996. *Structural studies of alkali metal adsorption and coadsorption on metal surfaces*. *Surf. Sci. Rep.*, 23, 43-171.
- DUBOIS, L. H., NUZZO, R.G., 1992. *Synthesis, structure, and properties of model organic surfaces*. *Annu. Rev. Phys. Chem.*, 43, 437-463.
- FOLKERS, J. P., LEIBNIS, P. E., WHITESIDES, G. M., DEUTCH, J., 1994. *Phase behavior of two-component self-assembled monolayers of alkanethiolates on gold*. *J. Phys. Chem.*, 98, 563-571.
- GUGAŁA-FEKNER, D., NIESZPOREK, J., SIENKO, D., 2015. *Adsorption of anionic surfactant at the electrode-NaClO<sub>4</sub> solution interface*. *Monatsh. Chem.* 146, 541-545.
- JOSYPCUK, B., FOJTA, M., JOSYPCHUK, O., 2013. *Thiolate monolayers formed on different amalgam electrodes. Part II: Properties and application*. *J. Electroanal. Chem.*, 694, 84-93.
- KLIN, M., NIESZPOREK, J., SIENKO, D., GUGAŁA-FEKNER, D., SABA, J., 2011. *Adsorption of tetramethylthiourea in the presence of cationic detergent at interface electrode/aqueous perchlorate solutions*. *Croat. Chem. Acta.* 84, 475-480.
- KUMAR, D., RUB, M.A., 2019. *Role of cetyltrimethylammonium bromide (CTAB) surfactant micelles on kinetics of [Zn(II)-Gly-Leu]<sup>+</sup> and ninhydrin*. *J. Mol. Liq.*, 274, 639-645.
- NOSAL-WIERCIŃSKA, A., 2010. *Adsorption of cystine at mercury/aqueous solution of chlorate (VII) interface in solutions of different water activity*. *Cent. Europ. J. Chem.*, 10, 1290-1300.
- NOSAL-WIERCIŃSKA, A., KALISZCZAK, W., GROCHOWSKI, M., WIŚNIEWSKA, M., KLEPKA, T., 2018. *Effect of mixed adsorption layers of 6-mercaptopurine-Triton X-100 and 6-mercaptopurine-Tween 80 on the double layer parameters at the mercury/chlorates (VII) interface*. *J. Mol. Liq.*, 253, 143-148.
- NOSAL-WIERCIŃSKA, A., MARTYNA, M., GROCHOWSKI, M., BAŚ, B., 2021. *First electrochemical studies on "CAP - PAIR" effect for Bi(III) ion electroreduction in the presence of 2-Thiocytosine on novel cyclically renewable liquid silver amalgam film electrode (R-AgLAFE)*. *J. Electrochem. Soc.*, 168, 066504.
- PAGAC, E. S., PRIEVE, D. C., TILTON, R. D., 1998. *Kinetics and mechanism of cationic surfactant adsorption and coadsorption with cationic polyelectrolytes at the silica-water interface*. *Langmuir*, 14, 2333-2342.
- SOTIROPULO, S., NIKITAS, P., PAPADOPOULO, N., 1993. *Interfacial micellization of cetyl-dimethylbenzylammonium chloride and Tween 80 at the Hg/electrolyte solution interphase*. *J. Electroanal. Chem.*, 356, 225-243.
- SZYMCZYK, K., ZDZIENNICKA, A., JAŃCZUK, B., 2015. *Adsorption and wetting properties of cationic, anionic and nonionic surfactants in the glass-aqueous solution of surfactant-air system*. *Mater. Chem. Phys.*, 162, 166-176.
- ULMAN, A., 1996. *Formation and structure of self-assembled monolayers*. *Chem. Rev.* 96, 1533-1554.